JOURNAL OF AIRCRAFT
Vol. 45, No. 6, November–December 2008

Shallow Rectangular Cavities at Low Speeds Including Effects of Yaw

S. L. Gai,* T. J. Soper,† and J. F. Milthorpe‡
University of New South Wales, Canberra, Australian Capital Territory 2600, Australia

DOI: 10.2514/1.37927

This paper presents a low-speed investigation of flow and drag characteristics of straight and shallow rectangular cavities including the effects of yaw. All the flow regimes of cavity flow, that is, "open," "transitional," and "closed" were investigated. Measurements consisted of pressure data (both mean and fluctuating) and oil flow visualization. It was found that with a cavity at zero yaw, the drag, based on the projected frontal area of the cavity, increased from open to closed. The effect of yaw was such that the relative drag of the cavity in all the flow regimes showed a decrease with increase in yaw angle. This decrease varied between 20 and 35% at the highest yaw angle (45 deg) tested.

Nomenclature

C_D	=	drag coefficient based on projected frontal area of cavity
C_f	=	skin friction coefficient
C_p	=	pressure coefficient
C_D^*	=	drag coefficient based on planform area of cavity
d	=	cavity depth, mm
f	=	frequency, Hz
l	=	cavity length, mm
m	=	mode number
M	=	Mach number
Re	=	Reynolds number
U	=	freestream velocity
w	=	width, mm
x, y, z	=	coordinates in the streamwise, vertical, and spanwise directions centered on the cavity axis and measured from the cavity front face
γ	=	time lag constant (defined in text)
δ	=	boundary layer thickness at the cavity leading edge, mm
θ	=	momentum thickness, mm
κ	=	ratio of convective speed of vortices to the freestream speed
ρ	=	density
ψ	=	yaw angle, deg
∞	=	infinity

Introduction

A BETTER understanding of cavity flows is beneficial because such flows are quite common on aircraft structures, for example, landing gear wells, storage of radar and photographic equipment for surveillance and reconnaissance, as well as weapons bays for store release [1]. Cavity flows are also important in continuous wave laser applications, ship hulls [2], and sunroofs and windows in automobiles [3]. In most subsonic and supersonic configurations, the presence of cavities has generally undesired effects. The cavities increase drag and give rise to oscillatory flows which can generate noise and vibration of structures that can eventually lead to fatigue and buffeting. In this paper we report on an investigation into drag of shallow rectangular cavities at yaw. There are very few studies available at present [4,5] that include effects of yaw on cavity flow, especially effects of yaw on drag. In quite a few instances, in practice, a cavity may be yawed to the main flow direction, either due to design constraints or due to the occurrence of crosswinds. When it is realized that aircraft excrescence drag can be as much as 3% of the total drag [4], the significance of understanding and attempts to reduce the drag due to cavities become obvious.

In the present investigation, we consider "shallow" cavities, wherein the length-to-depth ratio (l/d) of the cavity is much greater than unity [6]. The cavities are further classified [1] as "open," "transitional," or "closed" depending on their length-to-depth ratio l/d. An open cavity is one wherein the ratio l/d is usually less than 10. Such cavities typify bomb bays and landing gear wells of aircraft. With such cavities, the shear layer, which separates from the cavity leading edge, essentially bridges the cavity length. Although the mean pressure in the cavity is nearly uniform, the instabilities in the separated shear layer and the upstream traveling pressure waves that are generated as a result of the shear layer impingement onto the cavity rear wall produce self-sustaining pressure oscillations with sharp acoustic tones. These can give rise to vibrations of the structure which, in turn, can lead to buffeting and fatigue. If l/d is greater than about 13, the cavity is said to be closed. Such cavities typically represent missile bays. The flow in such cavities first separates at the cavity leading edge, reattaches on the cavity floor a short distance downstream, before separating in front of the cavity rear face and then attaching to the trailing edge of the cavity. The (mean) pressure distribution of such a flow yields a low pressure (compared to the pressure upstream of the cavity) in the forward part of the cavity followed by a near plateau, where the flow is attached and then a high pressure region at the rear where the flow is again attached at the trailing edge. The closed cavity generally does not produce strong self-sustaining pressure oscillations with acoustic tones. The cavities wherein $10 \leq l/d \leq 13$ are called transitional. Those that are at the lower end of this range are sometimes designated "transitional open" and those at the higher end "transitional closed" [7]. This distinction is less obvious at lower speeds where the transition from totally open to totally closed is more gradual [1]. In the present investigation, all these regimes are covered.

Experimental Details and Techniques

The experiments were conducted in an open circuit low-speed wind tunnel with a square test section of 457 mm × 457 mm at a

Received 8 April 2008; revision received 14 July 2008; accepted for publication 15 July 2008.

*Visiting Senior Research Fellow, School of Aerospace, Civil and Mechanical Engineering, University of New South Wales at Australian Defence Force Academy. Associate Fellow AIAA.

†Honors Student, School of Aerospace, Civil and Mechanical Engineering, University of New South Wales at Australian Defence Force Academy.

‡Senior Lecturer, School of Aerospace, Civil and Mechanical Engineering, University of New South Wales at Australian Defence Force Academy. Student Member AIAA.

freestream speed of 15 m/s. The Reynolds number at the cavity leading edge based on the test section length was 5.5×10^5 and the measured boundary layer thickness at the cavity leading edge was 20 mm. The boundary layer thickness was determined by traversing a pitot tube of 1 mm outer diameter and 0.5 mm internal diameter and connected to a micromanometer. The boundary layer was turbulent and close to the one-seventh power law profile. The Reynolds number based on the boundary layer momentum thickness was 1.33×10^4. As the boundary layer was turbulent, it was expected that the flow over the cavity would be fairly independent of the Reynolds number. The turbulence level in the tunnel was less than 0.3%. The full details of the tunnel are given in [8].

To create cavity models, one of the test section windows was modified to incorporate rectangular box cavity configurations. The basic cavity configuration had a length l of 128 mm and a width w of 285 mm, thus giving an aspect ratio of 2.22. This adequately satisfies the two-dimensionality criterion as suggested by Ahuja and Mendoza [9]. The cavity, which was milled into the circular window of thickness 18 mm, was 8 mm deep and this was kept constant throughout. Thus the maximum l/d obtainable was 16. To obtain l/d ratios of 6, 8, and 10, inserts of length 80, 64, and 48 mm were used. Cavities giving length-to-depth ratios consistent with open, transitional, and closed flow were thus made possible. The desired cavity yaw angle could be obtained simply by rotating the window with respect to the freestream direction.

It may be pointed out that in the present instance the boundary layer thickness-to-cavity-depth ratio is 2.5, whereas in the experiments of Tracy and Plentovich [1] it varied between 0.2 and 0.83. Charwat et al. [10] point out that, in general, an increase in the boundary layer thickness-to-cavity-depth ratio results in the "smoothing out" of pressure gradients in the cavity and that this is a consequence of the decrease in the momentum transfer to the cavity.

The cavity was provided with 34 pressure ports of 0.5 mm diameter, a total of 25 on the cavity floor and 7 on the cavity face. These pressure orifices on the cavity face were located across the cavity height in a staggered manner with respect to the cavity centerline at 1 mm pitch. The floor pressure ports were staggered with respect to the floor centerline. To obtain the pressure data on cavity front and rear faces, the cavity was simply rotated through 180 deg. This meant that when the cavity is so rotated, the longitudinal position of the leading edge varied depending on the cavity l/d ratio. This, in turn, meant that the boundary layer thickness was slightly different for cavities of different l/d ratios. However, this should not affect the results very significantly. The two additional pressure ports were located across the span at a distance of 132.5 mm with respect to the centerline on the cavity floor. These were used to provide a differential pressure measurement to set the cavity leading edge normal to the freestream at zero yaw. This procedure yielded a reliable estimate of 0 deg yaw as these pressure orifices were located from the tunnel sidewalls at least two boundary layer thicknesses away. The pressures were measured using a scanivalve system SSS 48C in conjunction with a Baratron MK 4 pressure transducer. This was connected to an interface unit and controlled via the scanivalve controller program running on a NEC Powermate 386 computer. Before testing, the scanivalve pressure transducer was calibrated using a Druck DPI 610 pressure calibrator accurate to ± 1 Pa. Overall, the pressure measurement system accuracy was of the order of $\pm 1\%$. The schematic of the model and pressure tap locations is shown in Fig. 1.

Fluctuating pressures were also measured using two analog KP101-A type transducers. One was used to measure the pressures on the cavity face and the other on the floor 32 mm from the cavity face. The output from the transducer was connected to a differential amplifier and the output of the amplifier was recorded on an oscilloscope. Once the voltage had been recorded, the data were processed on a computer. The transducers were temperature compensated.

A separate model was employed for oil flow visualization data. A mixture of kerosene and titanium dioxide with a few drops of oleic acid was chosen. A number of trials were necessary before the optimum proportion of the mixture was decided. This consisted of, by volume, 7 parts of kerosene, 1 part of titanium dioxide with 4 drops of oleic acid. The mixture was applied to the surface of the model using a fine paint brush. Once the tunnel had been run for a time, photographs were taken of the resulting streamlines using a digital camera.

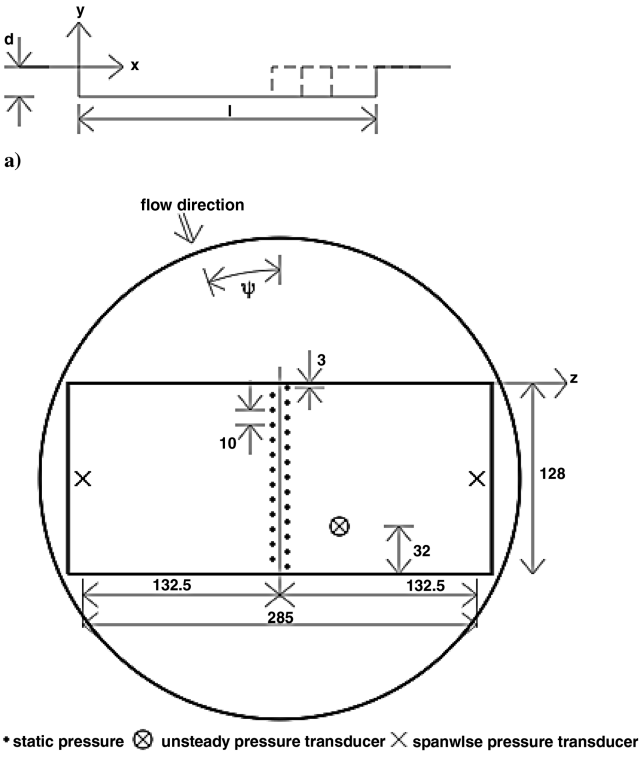

Fig. 1 Schematic of model and pressure tap locations. Dimensions are in millimeters.

Results and Discussion

Steady Pressure Distributions

Figure 2 shows steady pressure distributions in the cavity with $l/d = 6$. They are expressed in terms of the pressure coefficient C_p plotted against x/l, the distance along the cavity floor measured from the cavity leading edge normalized by the cavity length. The pressure distributions for zero yaw seem consistent with open cavity behavior as suggested by Tracy and Plentovich [1] in that the pressures are nearly constant over most of the cavity and increase as the rear face is approached. The effect of increasing yaw is to reduce the pressures both inside the cavity as well as near the cavity rear face. The large fluctuations observed in the distributions, particularly near the cavity rear face at larger yaw angles, are thought to be due to crossflow

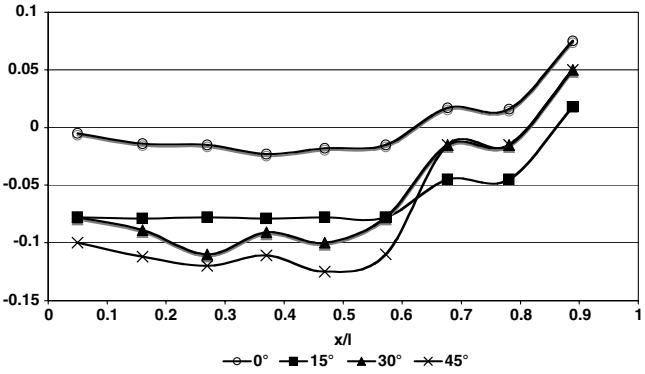

Fig. 2 Open cavity pressure distributions at various yaw angles, $l/d = 6$.

effects. This is confirmed by the oil flow visualizations as will be shown later.

Figure 3 shows the pressure distributions for a cavity with $l/d = 8$. Again at zero yaw, they are generally consistent with a transitional open-type distribution [1], wherein the constant pressure region extends only a short distance ($0 < x/l < 0.35$) from the leading edge and thereafter the pressure increases gradually up to the trailing edge. The effect of increasing yaw once again results in decreasing pressures throughout the cavity, and the unsteadiness of pressures near the trailing edge is due to the combined effect of flow impingement and crossflows. These results seem to indicate that the lower bound of transitional open type flow can occur for cavities with $l/d < 10$, the limit suggested by Tracy and Plentovich [1].

Figure 4 shows the results for a cavity with $l/d = 10$. The zero yaw distribution for this configuration is in the transitional closed regime according to Tracy and Plentovich [1]. Here there is a very short region ($0 < x/l < 0.3$) of nearly constant pressure immediately following the front face and then a gradual increase in pressure with a hint of a plateau in the midspan region of the cavity. Again, the pressure levels decrease with increase in yaw. The unsteadiness in pressures near the trailing edge, however, is less pronounced than for the open and transitional open cavities.

Figure 5 shows pressure distributions for a closed cavity with $l/d = 16$. The strong rise in pressures followed by a well-defined plateau and a subsequent rise as the trailing edge is approached are characteristic of the straight closed cavity pressure distribution as suggested by Tracy and Plentovich [1]. In a closed cavity, the shear layer after separation from the leading edge attaches to the cavity floor and then again separates as the cavity rear face is approached and finally reattaches to the trailing edge. As before, the effect of increasing yaw is to considerably reduce the pressures across the cavity length. The slight rise and then drop in pressures immediately after the leading edge is believed to be due to the impingement of the separation vortex against the cavity face. This feature is seen to consistently appear at all the yaw angles.

The marked fluctuations observed in pressure distributions for the open ($l/d = 6$) and transitional open ($l/d = 8$) cavities are

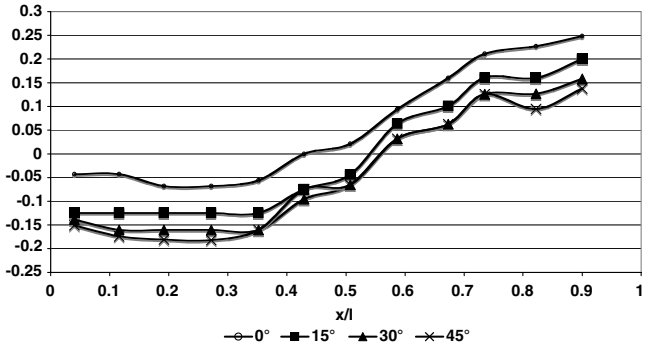

Fig. 3 Transitional open cavity pressure distributions at various yaw angles, $l/d = 8$.

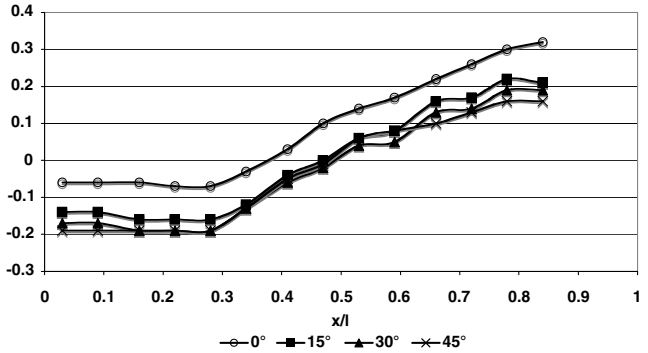

Fig. 4 Transitional closed cavity pressure distributions at various yaw angles, $l/d = 10$.

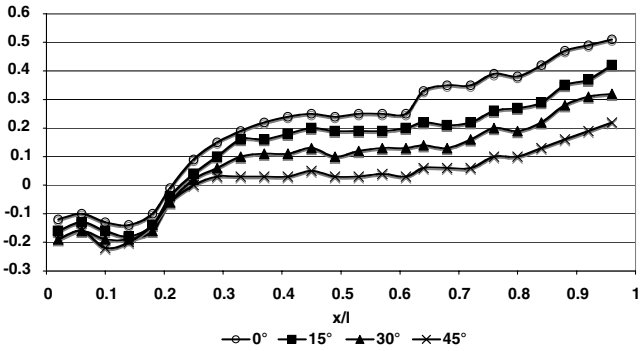

Fig. 5 Closed cavity pressure distributions at various yaw angles, $l/d = 16$.

considerably less for both closed ($l/d = 16$) and transitional closed ($l/d = 10$) cavities. This would suggest that crossflow effects may be less severe near the rear face in the case of closed and transitional closed cavities, because in these cavities the flow remains attached for a considerable distance along the cavity floor unlike in the case of open and transitional open cases. The other possibility is that both open and transitional open cavities can sustain cavity resonance although at these very low Mach numbers this may not be a dominant feature. This aspect will be discussed subsequently.

These pressure distributions at nonzero yaw angles are generally consistent with those of Plentovich et al. [11] whose investigation was restricted to yaw angles of 0 and 15 deg and Mach numbers between 0.2 and 0.9.

Oil Flow Visualization

Figures 6–8, show oil flow photographs of the cavity flows at 45-deg yaw angle. These tests were done mainly to confirm the pressure data. The results with 15-deg yaw angle showed very mild spanwise flows while the 30-deg yaw angle results were very similar to the 45 deg data, only slightly less severe. Hence they have not been included. Secondly, only the results for $l/d = 8$ are shown as those with $l/d = 10$ were very similar as can be seen by the pressure data of Figs. 3 and 4. There is also the possibility that at high angles of yaw, there may be vortices from the cavity leading edge that may interact with sidewalls and thereby contribute to sidewall/cavity flow interactions. However, it was not possible to specifically quantify these secondary effects.

Figure 6 shows the oil flow pattern for the open cavity ($l/d = 6$) at 45 deg yaw. The flow is from right to left. The rectangular boundaries of the cavity are clearly identifiable. We can recognize a separation region after the cavity leading edge, which becomes progressively large in the spanwise direction and the separation line becomes curved toward the sidewall indicating a strong interaction of cavity

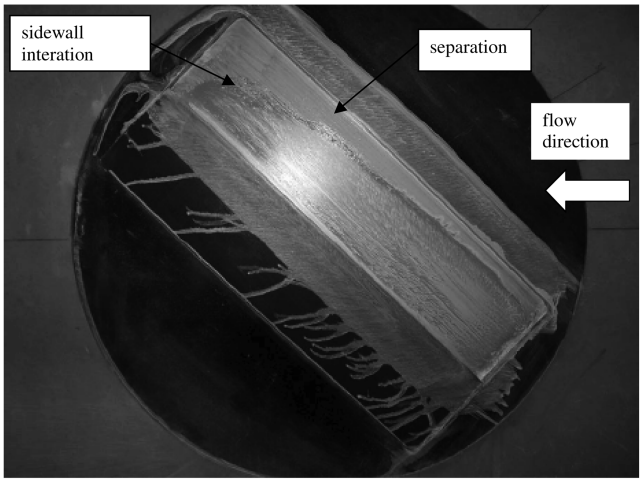

Fig. 6 Oil flow visualization for open cavity ($l/d = 6$) at 45 deg yaw.

flow with the sidewall toward the top left-hand corner. This strong interaction of crossflows with sidewall combined with flow impingement at the cavity rear face could possibly explain the fluctuations seen in pressure distributions (Fig. 2).

Figure 7 shows the flow pattern for the transitional closed cavity ($l/d = 8$) at 45 deg yaw. One can again identify a separation region following the leading edge. We also note the curved separation line toward the sidewall indicating a strong sidewall interaction. The flow picture is similar to the previous open cavity case.

Figure 8 is an illustration of closed cavity flow ($l/d = 16$) at 45 deg yaw. As in the previous photographs, we note the separation following the leading edge shows an increase in the spanwise direction and also strong impingement and sidewall interaction as seen at the top right-hand corner. In addition, we also note that the crossflows are not predominantly parallel to the edges but merge into the separation line in front of the cavity rear face. A distinct separation region in front of the rear face can be identified. The midspan region shows an attached flow dominated by both streamwise and crossflows.

Unsteady Pressures and Spectra

As stated in the section Experimental Details and Techniques, the two KPA-101A pressure transducers were used to measure fluctuating pressures within the open cavity that had a length-to-depth ratio of 6.

Tracy and Plentovich [1] noted sharp resonant peak amplitudes with open cavities while closed and transitional cavities generally displayed a broadband spectra. The sharpness and amplitude of the spectra were also found to be dependent on the Mach number. The spectra obtained here with the straight open cavity ($\psi = 0$ deg) with $l/d = 6$ do give an indication of peaks in the frequency range 62.5 Hz $\leq f \leq$ 468.75 Hz as seen in Fig. 9. However, as has been suggested in [1], at this very low Mach number, the resonant frequencies are not sharp and distinct. This is also supported by the recent low-speed shallow cavity data of Daoud et al. [12]. The progressive reduction in sharpness of the peaks at higher frequencies with lower fluctuating pressure levels is also indicative of the more broadband nature of pressure fluctuations. Thus, although the peaks indicated in the above spectra are no guarantee that self-sustaining cavity oscillations exist, it was instructive to verify if they were Rossiter modes [13] and compare them with his semi-empirical theory. Rossiter's expression is

$$\frac{fl}{U} = \frac{m - \gamma}{M + (1/\kappa)}$$

where the symbols are as defined in the nomenclature. In this expression, κ is the ratio of convective velocity of vortices to the freestream velocity, which was assumed by Rossiter to be 0.57. γ is a constant defining the time lag between the arrival of the vortex at the cavity trailing edge and the emission of the main acoustic pulse directed toward the upstream leading edge. Rossiter assumes $\gamma =$ 0.25 based on experimental data. The veracity of the Rossiter formula has been confirmed by many researchers.

Figure 10 shows this comparison. Here the experimental values for modes $m = 1$, 2, 3, and 4 are compared with those calculated using the Rossiter formula [13]. The straight line through the experimental data has a slope of 0.71 instead of the ideal value of unity. Also shown are the data of Tracy and Plentovich [1] for an open cavity of $l/d = 6$ at $M_\infty = 0.2$, the lowest freestream Mach number in their experiments. It has a slope of 1.13. These data suggest that a Rossiter-type resonance might be occurring in the present case although the freestream Mach number (0.044) here is much smaller. Daoud et al. [12] discuss, at some length, the

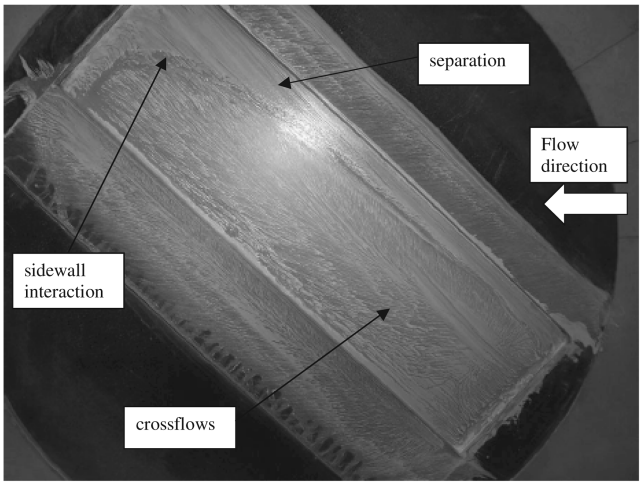

Fig. 7 Oil flow visualization for transitional open cavity ($l/d = 8$) at 45 deg yaw.

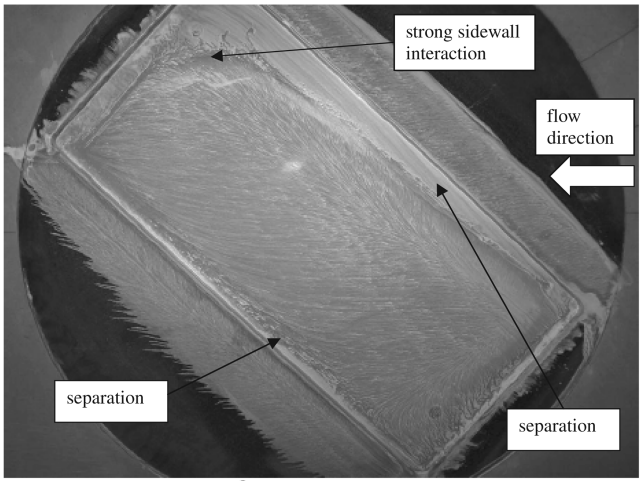

Fig. 8 Oil flow visualization for closed cavity ($l/d = 16$) at 45 deg yaw.

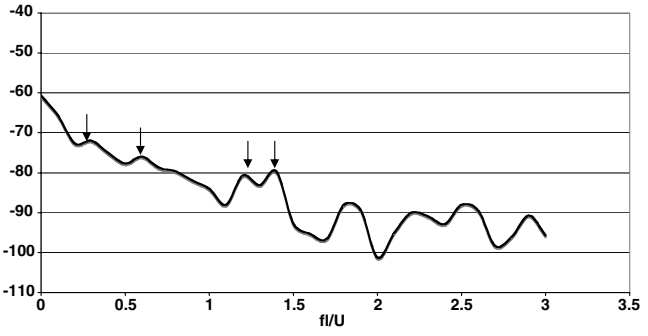

Fig. 9 Unsteady pressure spectra for straight ($\psi = 0$ deg) open cavity of $l/d = 6$.

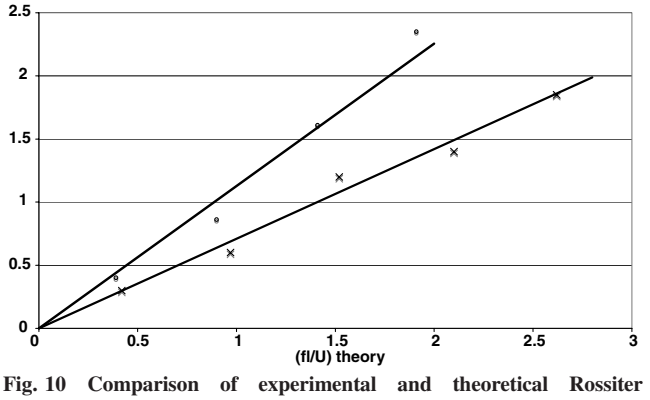

Fig. 10 Comparison of experimental and theoretical Rossiter frequencies for $l/d = 6$ at low speeds. times: present data; circle: Tracy and Plentovich [1].

conditions for the existence of Rossiter modes in very low Mach number cavity flows. They point out that for Rossiter modes to exist, the cavity length must exceed a certain minimum threshold given by $l_{\min} \approx 800\theta Re_\theta^{-1/2}$ based on the earlier work by Sirohia [2] and Gharib and Roshko [14]. Here θ is the momentum thickness of the separating boundary layer at the cavity leading edge and Re_θ is the Reynolds number based on the momentum thickness. Based on this criterion, for the present experimental conditions, the minimum l/d ratio should be 1.7. Therefore, Rossiter modes are possible. Daoud et al. [12] also defined conditions for the so-called "wake mode" oscillations to exist in cavity flows. Accordingly, the criterion for wake modes to be possible, the minimum cavity length needs to be at least 75θ, which in the present instance would imply a cavity of $l/d = 18$. Thus, it is very unlikely that the wake mode oscillations would occur in any of the cavities tested herein.

The pressure spectra of this cavity at different angles of yaw showed only weak broadband levels with no discernible peaks. The results for transitional and closed cavities for all yaw angles were also broadband with no resonant peaks. The Tracy and Plentovich [1] data also show that pressure spectra are mainly broadband for transitional and closed cavities.

Cavity Drag

Following the approach by Squire and Nasser [15], we can represent the drag results in terms of the ratio C_D/C_f where C_D, the cavity pressure drag, is based on the projected *frontal* area of the cavity and C_f is the skin friction on the surface at the cavity position in the absence of the cavity. Then, this ratio corresponds to the cavity pressure drag to the friction drag based on the same projected frontal area. The skin friction C_f was calculated using the flat-plate turbulent skin friction relation of White [16]

$$C_f = \frac{0.455}{[\ell n(0.06Re_x)]^2}$$

where Re_x is the Reynolds number based on the distance to the leading edge of the cavity and freestream conditions. Squire and Nasser [15] point out that it is conventional to present the shallow cavity drag in this form as this quantifies the oft stated fact that the skin friction drag is much smaller and insignificant compared to the cavity pressure drag [10].

The cavity pressure drag C_D was calculated using the average values of the seven pressure ports on the two cavity faces with the assumption that this mean value acted on the whole face. Admittedly, this is an approximation which becomes questionable especially when the cavity is at yaw and C_D then measures the chordwise or normal (to the leading edge) component of the total drag. However, as the aspect ratio (w/d) is nearly 36, it is believed that the centerline values are not severely affected by sidewall effects. Savory et al. [4] found that the effect of yaw on the overall drag coefficient of a cavity was reduced as the cavity became more two dimensional (that is, increased in span). This they attributed to reduced endwall effects. They also found that the drag coefficient remained largely constant for yaw angles up to 30 deg.

Figure 11 shows the drag variation of straight cavities ($\psi = 0$ deg) in terms of C_D/C_f plotted against the depth-to-length ratio d/l. As noted by Squire and Nasser [15], variations in the drag coefficient based on the projected frontal area are more revealing when plotted against d/l. We note that the drag increases monotonically as the cavity regime changes from open to closed and a mean line through the data points shows a nearly linear relationship. Although the general relationship between C_D/C_f and d/l is nonlinear as shown by Squire and Nasser [15], within the small range of values of d/l covered here, it appears linear.

Next, it is also worthwhile to compare these results in terms of C_D^*/C_f where C_D^* is the drag coefficient based on the *plan* area of the cavity, again, as suggested by Squire and Nasser [15]. Figure 12 shows these results for the straight cavity ($\psi = 0$ deg). We note that C_D^*/C_f initially increases from the open cavity case reaching a maximum for the transitional open cavity and then gradually decreases as the cavity becomes fully closed. In fact, the values of C_D^*/C_f for fully open and fully closed cavities are almost the same with C_D^* approximately $11C_f$ for the open cavity and $12C_f$ for the closed cavity. This is consistent with the findings of Squire and Nasser who also found that maximum drag occurs for cavities with l/d ratios between 8 and 12.

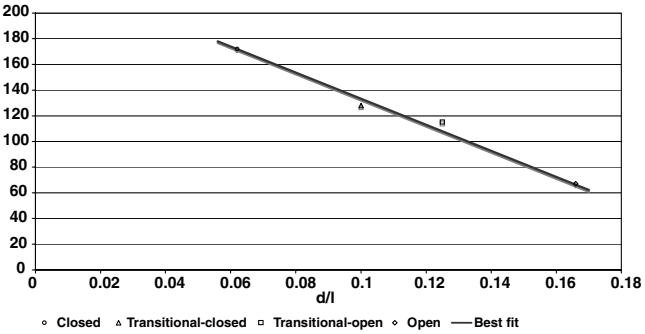

Fig. 11 Variation of C_D/C_f with cavity d/l.

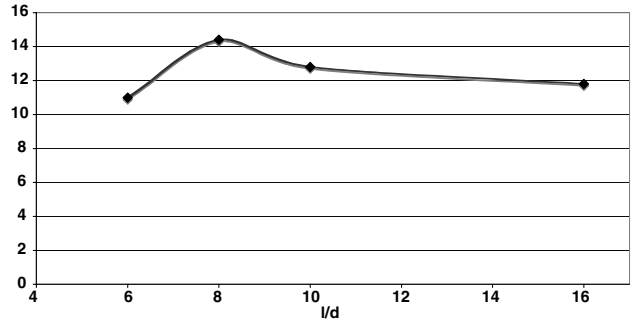

Fig. 12 Variation of C_D^*/C_f for straight ($\psi = 0$ deg) rectangular cavities of different l/d.

The effects of yaw are shown in Fig. 13. It is seen that relatively the drag decreases with increase in yaw for all the cavities. Secondly, although the drag reductions of different cavities show considerable scatter, they generally seem close to the cosine variation of the yaw angle ψ (solid line). Also shown on the figure (broken line) is the theoretical $\cos^2\psi$ variation of the normal component of the total drag force for an *infinite* span cavity in the spirit of Jones [17]. It is seen that the agreement seems better with the simple cosine variation than the theoretical $\cos^2\psi$ variation. This may be attributed to the fact that the cavity aspect ratio is finite in these experiments whereas the theory assumes infinite span. These results seem to indicate that the effect of crossflows is such as to reduce the impingement effect of the shear layers onto the cavity trailing edge, which would result in the reduction in the magnitude of the pressures on the cavity rear face, thus causing a reduction in drag. This is also confirmed from the

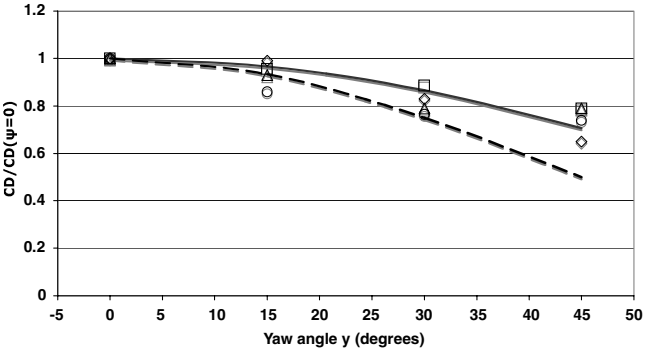

Fig. 13 Variation of $C_D^*/C_{D,\psi=0}^*$ with yaw angle ψ. circle: $l/d = 6$; triangle: $l/d = 8$; square: $l/d = 10$; diamond: $l/d = 16$; solid line: cos ψ; broken line: $\cos^2\psi$.

mean pressure data that, as the yaw angle is increased, the pressure levels, particularly on the rear face, decrease. The strong spanwise effects seen from the oil flow tests also support this possibility.

A comment needs to be made about these results when comparing with the low-speed data of Savory et al. [4] and Czech et al. [5]. These authors found that there was an increase in drag with yaw angle up to about 60 deg and then a steep decrease. However, it needs to be noted that in both their experiments the cavities were deep with $l/d = 2$ and $w/l = 2$. The cavity configuration in their case was thus strongly three dimensional and included the contribution of sidewall effects to the total drag. In the present case, the contributions of the tunnel sidewall effects are not included as there was no provision for the measurement of pressures on the sidewalls. The results, therefore, pertain to drag force normal to the cavity leading edge. Also, in the present experiments, the cavities are quite shallow with $0.0625 \leq d/l \leq 0.166$ and the aspect ratio w/l varied from 5.93 to 2.2. The approach suggested by Squire and Nasser [15] in the determination of drag of shallow cavities is hence justified for yaw angles less than 30 deg when the crossflow component of the total drag seems to be less than about 15%.

Conclusions

The steady pressure distributions at zero yaw were found to be consistent with open, transitional, and closed cavity configurations as shown by previous studies.

The effect of yaw on steady pressure distributions was such as to reduce the pressure levels throughout the cavity, this effect increasing with increase in the yaw angle.

The oil flow studies showed strong crossflows and sidewall interactions particularly at higher yaw angles.

The unsteady pressure spectra showed that the open cavity at zero yaw generates Rossiter-type self-sustaining resonant tones although these tones were not very sharp and distinct. The agreement between the experimental Strouhal frequencies and those calculated using the Rossiter formula was fair at best. This feature of low-speed open cavity flow is consistent with previous observations. The spectra for transitional and closed cavities were all broadband with no well-defined resonant tones. The effect of yaw for all cavities was to yield only a broadband spectra.

At zero yaw, the study showed that the cavity pressure drag, based on the projected frontal area and normalized with the skin friction drag, increased as the cavity flow regime changed from open to transitional to fully closed.

However, when the drag is expressed in terms of the cavity plan form area, the zero yaw drag initially increased from the open cavity flow regime reaching a maximum for the transitional open flow cavity and then showed a gradual decrease toward the fully closed cavity regime.

With increase in yaw, the drag component normal to the cavity leading edge showed a decrease for all cavity configurations. Although the data showed a considerable scatter, there was a trend toward a cosine variation of the yaw angle. These drag reductions were less than about 15 to 20% for yaw angles up to 30 deg and no more than 35% even at the highest yaw angle tested.

References

[1] Tracy, M. B., and Plentovich, E. B., "Cavity Unsteady-Pressure Measurements at Subsonic and Transonic Speeds," NASA TP 3669, Dec. 1997.

[2] Sarohia, V., "Experimental Investigation of Oscillations in Flows Over Shallow Cavities," *AIAA Journal*, Vol. 15, No. 7, 1977, pp. 984–991. doi:10.2514/3.60739

[3] Kook, H., Mongeau, L., Brown, D. V., and Zorea, S., "Analysis of the Interior Pressure Oscillations Induced by Flow over Vehicle Openings," *Noise Control Engineering Journal*, Vol. 45, No. 6, 1997, pp. 223–234. doi:10.3397/1.2828444

[4] Savory, E., Toy, N., Disimile, P. J., and Dimico, R. G., "The Drag of Three-Dimensional Rectangular Cavities," *Journal of Applied Scientific Research*, Vol. 50, 1993, pp. 325–346.

[5] Czech, M., Savory, E., Toy, N., and Mavrides, T., "Flow Regimes Associated with Yawed Rectangular Cavities," *The Aeronautical Journal*, Vol. 105, March 2001, pp. 125–134.

[6] Howe, M. S., *Acoustics of Fluid-Structure Interactions*, Cambridge Univ. Press, Cambridge, England, U.K., 1998.

[7] Plentovich, E. B., Stallings, R. L., and Tracy, M. B., "Experimental Cavity Measurements at Subsonic and Transonic Speeds," NASA TP 3358, 1993.

[8] Petrusma, M. S., "A Near Wake Study of Segmented Blunt Trailing Edge Aerofoils in Subsonic Flow," Ph.D. Thesis, University of New South Wales, Sydney, Australia, 1990.

[9] Ahuja, K. K., and Mendoza, J., "Effects of Cavity Dimensions, Boundary Layer, and Temperature on Cavity Noise with Emphasis on Benchmark Data to Validate Computational Aeroacoustic Codes," NASA CR 4653, 1995.

[10] Charwat, A. F., Roos, J. N., Dewey, C. F., and Hitz, J. A., "An Investigation of Separated Flows—Part 1: Pressure Field," *Journal of Aerospace Sciences*, Vol. 28, No. 6, 1961, pp. 457–470.

[11] Plentovich, E. B., Chu, J., and Tracy, M. B., "Effects of Yaw Angle and Reynolds Number on Rectangular-Box Cavities at Subsonic and Transonic Speeds," NASA TP 3099, 1991.

[12] Daoud, M., Naguib, A. M., Bassioni, I., Abdelkhalek, M., and Ghoniem, Z., "Microphone-Array Measurements of the Floor Pressure in a Low Speed Cavity Flow," *AIAA Journal*, Vol. 44, No. 9, 2006, pp. 2018–2023. doi:10.2514/1.18129

[13] Rossiter, J., "Wind Tunnel Experiments on the Flow over Rectangular Cavities at Subsonic and Transonic Speeds," Aeronautical Research Council, R& M 3438, 1964.

[14] Gharib, M., and Roshko, A., "The Effects of Flow Oscillations on Cavity Drag," *Journal of Fluid Mechanics*, Vol. 177, 1987, pp. 501–530. doi:10.1017/S002211208700106X

[15] Squire, L. C., and Nasser, S. H., "Cavity Drag at Transonic Speeds," *The Aeronautical Journal*, Vol. 97, Aug./Sept. 1993, pp. 247–256.

[16] White, F. M., *Viscous Fluid Flow*, 2nd ed., McGraw–Hill, New York, 1991.

[17] Jones, R. T., *Wing Theory*, Princeton Univ. Press, Princeton, NJ, 1990.